

Design of Serially Concatenated Codes based on Iterative Decoding Convergence

S. ten Brink

Institute of Telecommunications (Dep. 0408), University of Stuttgart
Pfaffenwaldring 47, 70569 Stuttgart, Germany, E-mail: tenbrink@inue.uni-stuttgart.de

Abstract: *The design of serially concatenated codes has yet been dominated by optimizing asymptotic slopes of error probability curves. We propose mutual information transfer characteristics for soft in/soft out decoders to design serially concatenated codes based on the convergence behavior of iterative decoding. The exchange of extrinsic information is visualized as a decoding trajectory in the Extrinsic Information Transfer Chart (EXIT chart).*

Keywords: serially concatenated codes, iterative decoding, convergence, mutual information

1. Introduction

Bit error rate (BER) charts of iterative decoding schemes exhibit a turbo cliff region [1] where commonly used bounding techniques fail to provide further guidelines for code design. This paper proposes extrinsic information transfer characteristics based on mutual information to describe the flow of extrinsic information through the soft in/soft out decoders. This proves to be particularly useful for optimizing serially concatenated codes [2] in the turbo cliff region. A decoding trajectory visualizes the exchange of extrinsic information between inner and outer decoder in the Extrinsic Information Transfer Chart (EXIT chart). In [3] the EXIT chart was introduced to provide design guidelines for constituent codes of parallel concatenated codes (PCC). In this paper we extend these results to serially concatenated codes (SCC). We do not claim to present a rigorous proof of stability and convergence of iterative decoding; however, simulation results suggest that the EXIT chart predicts the best possible convergence behavior of the iterative decoder for large interleaving depth.

2. Extrinsic Transfer Characteristics

2.1. Iterative Decoding of SCC

The iterative decoder for SCC is shown in Fig. 1. For each iteration, the inner decoder (BCJR algorithm [4]) takes channel observations Z and *a priori* knowledge A_1 on the inner information bits and outputs soft values D_1 . The extrinsic and channel information $E_1 = D_1 - A_1$ is passed through the

bit deinterleaver to become the *a priori* input A_2 for the outer decoder. The outer decoder feeds back extrinsic information $E_2 = D_2 - A_2$ which becomes the *a priori* knowledge A_1 for the inner decoder. The variables Z , A_1 , D_1 , E_1 , A_2 , D_2 and E_2 denote log-likelihood ratios (L-values [5]). In this paper we restrict ourselves to an overall code rate of $R = R_1 \cdot R_2 = 1 \cdot 1/2 = 1/2$, and thus all E_b/N_0 -values are given with respect to an $R = 1/2$ code.

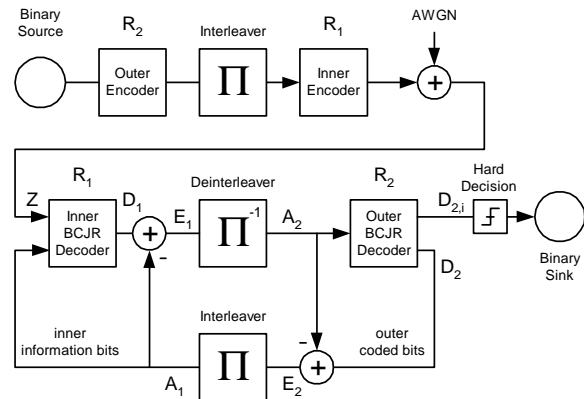


Figure 1: Encoder, channel and iterative decoder.

2.2. Transfer Characteristics of the Inner Decoder

The inputs to the inner decoder are the noise-corrupted channel observations Z and the *a priori* knowledge A_1 on the inner information bits. The decoder outputs extrinsic and channel information E_1 . From simulations of the iterative decoder we observed that the extrinsic information L-values E_2 (i. e. A_1) as fed back from the outer decoder are almost Gaussian distributed. Additionally, large interleavers keep the *a priori* L-values A_1 fairly uncorrelated over many iterations. Hence, it seems appropriate to model the *a priori* input A_1 as an independent Gaussian random variable n_{A_1} with variance $\sigma_{A_1}^2$ and mean zero. In conjunction with the known transmitted inner information bits $x \in \{\pm 1\}$ we write

$$A_1 = \mu_{A_1} \cdot x + n_{A_1}. \quad (1)$$

Since A_1 is supposed to be an L-value based on Gaussian distributions it can be shown [5] that μ_{A_1} must fulfill $\mu_{A_1} = \sigma_{A_1}^2/2$, and thus the conditional probability density function (PDF) is

$$p_{A_1}(\xi|X=x) = \frac{e^{-\frac{(\xi - \frac{\sigma_{A_1}^2}{2} \cdot x)^2}{2\sigma_{A_1}^2}}}{\sqrt{2\pi} \sigma_{A_1}}. \quad (2)$$

To measure the information content of the *a priori* knowledge, mutual information $I_{A_1} = I(X; A_1)$, $0 \leq I_{A_1} \leq 1$, between transmitted inner information bits X and the L-values A_1 is used [6].

$$I_{A_1} = \frac{1}{2} \cdot \sum_{x=-1,1} \int_{-\infty}^{+\infty} p_{A_1}(\xi|X=x) \times \text{ld} \frac{2 \cdot p_{A_1}(\xi|X=x)}{p_{A_1}(\xi|X=-1) + p_{A_1}(\xi|X=1)} d\xi \quad (3)$$

With (2), equation (3) becomes

$$I_{A_1}(\sigma_{A_1}) = \int_{-\infty}^{+\infty} \frac{e^{-\frac{(\xi - \sigma_{A_1}^2/2)^2}{2\sigma_{A_1}^2}}}{\sqrt{2\pi} \sigma_{A_1}} \cdot (1 - \text{ld} [1 + e^{-\xi}]) d\xi. \quad (4)$$

For abbreviation we define

$$J(\sigma) := I_{A_1}(\sigma_{A_1} = \sigma) \quad (5)$$

$$\lim_{\sigma \rightarrow 0} J(\sigma) = 0, \quad \lim_{\sigma \rightarrow \infty} J(\sigma) = 1, \quad \sigma > 0 \quad (6)$$

The function $J(\sigma)$ cannot be expressed in closed form. It is monotonically increasing and thus reversible. Mutual information is also used to quantify the extrinsic output $I_{E_1} = I(X; E_1)$; it is computed according to (3), but now using the extrinsic output PDF p_{E_1} . Viewing I_{E_1} as a function of I_{A_1} and the E_b/N_0 -value, the inner extrinsic information transfer characteristics are defined as

$$I_{E_1} = T_1(I_{A_1}, E_b/N_0). \quad (7)$$

To calculate the characteristic $T_1(I_{A_1}, E_b/N_0)$ for a desired $(I_{A_1}, E_b/N_0)$ -input combination, the distributions p_{E_1} are most conveniently determined by means of Monte Carlo simulation. For this, the independent Gaussian random variable of (1) with $\sigma_{A_1} = J^{-1}(I_{A_1})$ is applied as *a priori* input to the inner decoder of interest. Fig. 2 shows transfer characteristics of some inner rate 1 (i. e. all coded bits) recursive convolutional codes at $E_b/N_0 = 1\text{dB}$ with feedback polynomial G_r and feedforward polynomial G . For most codes with G being different from a power of two, we find $I_{E_1}(I_{A_1} = 0) \approx 0$ which makes them inappropriate for use as inner codes in an iterative decoding scheme, as will become more obvious in Section 3.

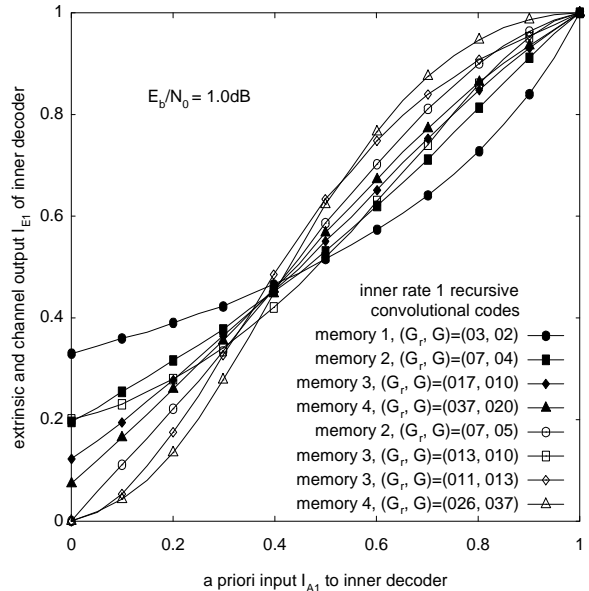


Figure 2: Extrinsic information transfer characteristics of some inner rate 1 decoders at $E_b/N_0 = 1\text{dB}$.

2.3. Transfer Characteristics of the Outer Decoder

The outer extrinsic transfer characteristic is

$$I_{E_2} = T_2(I_{A_2}) \quad (8)$$

and describes the input/output relationship between outer coded input A_2 , and outer coded extrinsic output E_2 . It is not dependent on the E_b/N_0 -value. It can be computed by assuming A_2 to be Gaussian distributed and applying the same equations as presented for T_1 in Section 2.2.

Extrinsic transfer characteristics of rate 1/2 codes for a wide range of different memories are given in Fig. 3. The legend in the upper left corner denotes systematic block codes of different lengths ($N - K$ parity checks), the legend in the lower right corner recursive systematic convolutional codes. It is straightforward to show that the transfer characteristic of an outer repetition code is $I_{E_2} = I_{A_2}$ (diagonal line). All transfer characteristics seem to cross in a single point at (0.5, 0.5). Note that the axes are swapped: I_{A_2} is on the ordinate, I_{E_2} on the abscissa.

3. Extrinsic Information Transfer Chart

To visualize the exchange of extrinsic information, we plot both decoder characteristics into a single diagram, which is referred to as Extrinsic Information Transfer Chart. On the ordinate, the inner extrinsic and channel output I_{E_1} becomes the outer *a priori* input I_{A_2} (interleaving does not change mutual information). On the abscissa, the outer extrinsic output I_{E_2} becomes the inner *a priori* in-

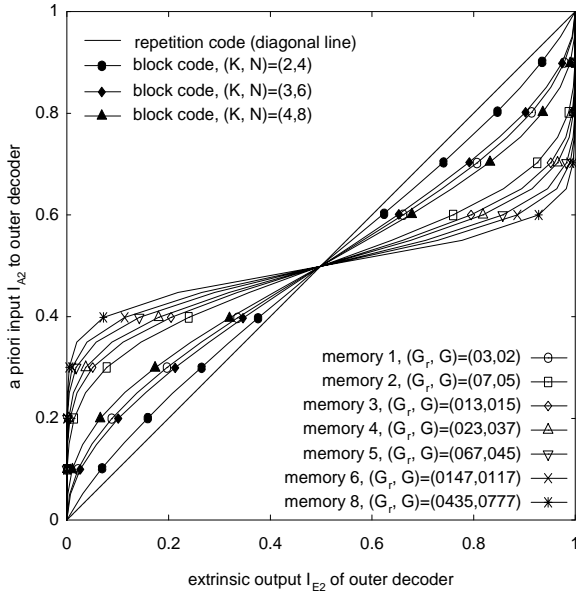


Figure 3: Extrinsic information transfer characteristics of some outer rate 1/2 decoders.

put I_{A_1} . Provided that independence and Gaussian assumptions hold for modelling extrinsic information (*a priori* information respectively), the transfer characteristics of Section 2 should approximate the true behavior of the iterative decoder. Moreover, the decoding trajectory that can be graphically obtained by simply drawing a zigzag-path into the EXIT chart (bounded by the decoder transfer characteristics) should match with the trajectory computed by simulations.

Fig. 4 shows trajectories of iterative decoding at $E_b/N_0 = 1\text{dB}$, 1.1dB and 1.5dB as obtained from simulations of the iterative decoder. For this example, the code concatenation consists of an inner differential encoder and an outer rate 1/2 recursive systematic convolutional code of memory 2. Note that the inner and outer transfer characteristics are just taken from Fig. 2 and Fig. 3. For $E_b/N_0 = 1\text{dB}$ the trajectory gets stuck after about four iterations since both decoder characteristics do intersect. For $E_b/N_0 = 1.1\text{dB}$ the inner transfer characteristic has been raised just high enough to open a narrow tunnel for the trajectory to “sneak through” and to converge towards low BER ($\approx 10^{-6}$). At $E_b/N_0 = 1.5\text{dB}$, less iterations are needed to converge towards low BER. This “turbo cliff”-effect is illustrated by the corresponding BER chart in the lower right corner.

The simulated trajectories match with the characteristics very well, owing to the large interleaver which ensures that the independence assumption of (1) holds over many iterations; in addition to that, the robustness of the mutual information measure allows to overcome non-Gaussian distributions of *a*

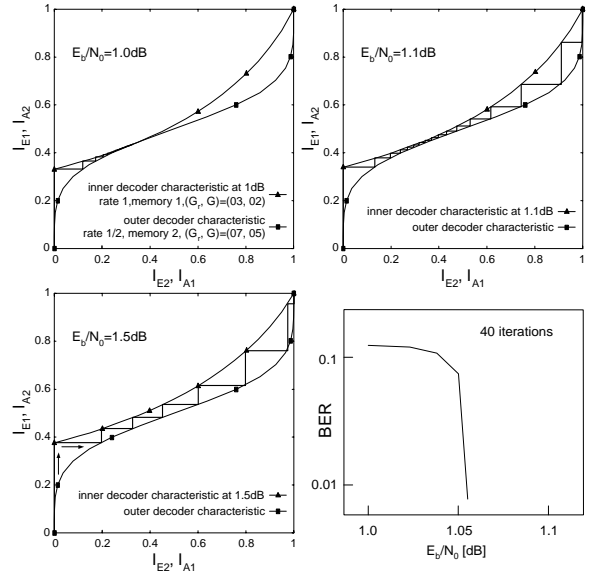


Figure 4: EXIT charts with iterative decoding trajectories at $E_b/N_0 = 1\text{dB}$, 1.1dB and 1.5dB ; corresponding BER chart; interleaver size 400000 outer coded bits.

priori information. It should be emphasized, however, that the *decoding trajectory* is a simulation result purely based on measurements of mutual information as taken from the output of the respective decoder. Only to calculate the *transfer characteristics* of individual decoders we were sought to impose the Gaussian and independence assumption on the *a priori* inputs A_1 , A_2 .

4. Code Design with the EXIT Chart

The code concatenation of Fig. 4 has its turbo cliff slightly above 1dB . In this Section we modify the inner and outer codes of our previous example to study the convergence properties of the new concatenation in the EXIT chart.

We observed that one can raise the beginning of the inner decoder transfer characteristic (at the cost of sacrificing a little towards the end) by substituting every other coded bit by its systematic counterpart to obtain a “systematically doped” inner recursive convolutional code of rate 1 with half of the bits being systematic. Then, convergence is already possible at 1dB (Fig. 5). For comparison, the transfer characteristic of the “undoped” inner code is given as a dashed line.

Another alternative to lower the turbo cliff position of the code concatenation of Fig. 4 is to steepen the slope of the outer characteristic by, e. g., using the rate 1/2 block code of length $N = 8$ coded bits of Fig. 3. Then we achieve convergence at 1dB as well (Fig. 6). For comparison, the transfer characteristic of the outer memory 2 convolutional code is given as

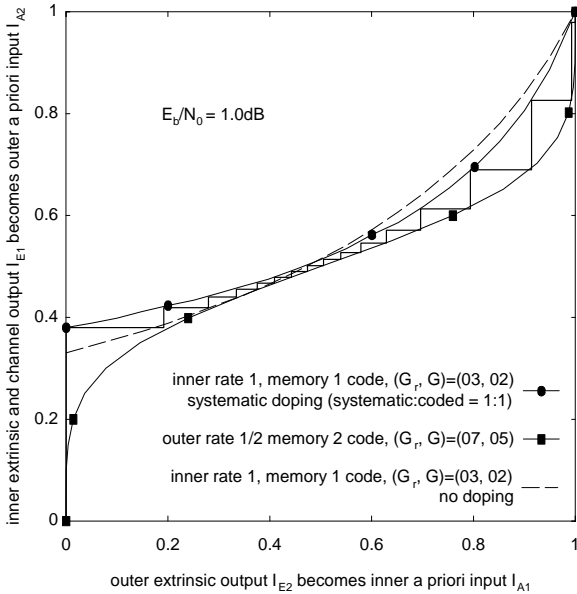


Figure 5: EXIT chart with decoding trajectory at $E_b/N_0 = 1\text{dB}$; inner systematically doped code; interleaver size 400000 outer coded bits.

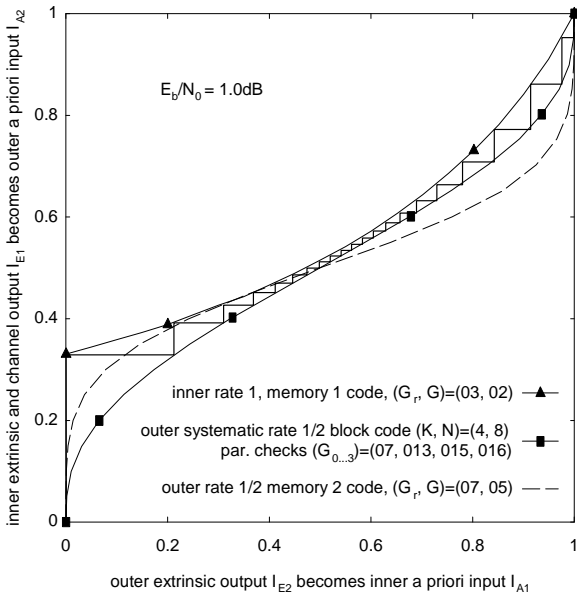


Figure 6: EXIT chart with decoding trajectory at $E_b/N_0 = 1\text{dB}$; outer block code; interleaver size 400000 outer coded bits.

a dashed line.

We performed a code search over inner rate 1 recursive convolutional codes up to memory 6. In combination with an outer repetition code (diagonal line in EXIT chart), a code with “early” convergence turns out to be of memory 4, with polynomials $(G_r, G) = (037, 020)$. A turbo cliff just below 0.5dB demonstrates that we can find SCC with iterative decoders operating close to Shannon’s capacity limit

(0.19dB). As the code search was performed based on transfer characteristics of *individual inner codes*, we verified the results by simulating the corresponding *iterative decoder* (see decoding trajectory at 0.5dB in Fig. 7). Contour lines indicate where a BER of 0.1, 0.01 and 0.001 is reached, compare to (23) of [3].

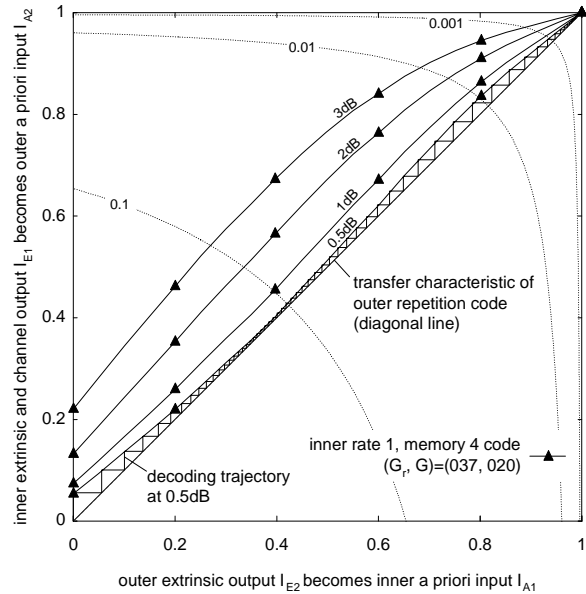


Figure 7: EXIT chart with iterative decoding trajectory at $E_b/N_0 = 0.5\text{dB}$; outer repetition code; interleaver size 400000 outer coded bits.

REFERENCES

- [1] C. Berrou, A. Glavieux, P. Thitimajshima, “Near Shannon limit error-correcting coding and decoding: Turbo-codes”, *Proc. ICC*, pp. 1064–1070, May 1993
- [2] S. Benedetto, D. Divsalar, G. Montorsi, F. Pollara, “Serial Concatenation of Interleaved Codes: Performance Analysis, Design, and Iterative Decoding”, *IEEE Trans. Inform. Theory*, vol. 44, no. 3, pp. 909–926, May 1998
- [3] S. ten Brink, “Iterative Decoding Trajectories of Parallel Concatenated Codes”, *Proc. 3rd IEEE/ITG Conference on Source and Channel Coding*, pp. 75–80, Munich, Jan. 2000
- [4] L. Bahl, J. Cocke, F. Jelinek, J. Raviv, “Optimal decoding of linear codes for minimizing symbol error rate”, *IEEE Trans. Inform. Theory*, vol. 20, pp. 284–287, Mar. 1974
- [5] J. Hagenauer, E. Offer, L. Papke, “Iterative Decoding of Binary Block and Convolutional Codes”, *IEEE Trans. Inform. Theory*, vol. 42, no. 2, pp. 429–445, Mar. 1996
- [6] T. M. Cover, J. A. Thomas, *Elements of Information Theory*. Wiley, New York, 1991.